

Fluxon-semi-uxon interaction in an annular long Josephson 0- π -junctionE. G. Oldobin,¹ N. Stefanakis,² D. Koelle,¹ and R. Kleiner¹¹ Physikalisches Institut { Experimentale Physik II, Universität Tübingen,

Auf der Morgenstelle 14, D-72076 Tübingen, Germany

² Institut für Theoretische Physik, Universität Tübingen,

Auf der Morgenstelle 14, D-72076 Tübingen, Germany

(Dated: February 21, 2022)

We investigate theoretically the interaction between integer and half-integer Josephson vortices (uxons and semi-uxons) in an annular Josephson junction. Semi-uxons usually appear at the 0- π -boundary where there is a π -discontinuity of the Josephson phase. We study the simplest, but the most interesting case of one π -discontinuity in a loop, which can be created only artificially. We show that measuring the current-voltage characteristic after injection of an integer uxon, one can determine the polarity of a semi-uxon. Depending on the relative polarity of uxon and semi-uxon the static configuration may be stable or unstable, but in the dynamic state both configurations are stable. We also calculate the depinning current of N uxons pinned by an arbitrary fractional vortex.

PACS numbers: 74.50.+r, 85.25.Cp, 74.20.Rp

Keywords: Long annular Josephson junction, sine-Gordon, half-integer ux quantum, semi-uxon, 0- π -junction

I. INTRODUCTION

For conventional Josephson junctions the first Josephson relation reads $I_s = I_c \sin(\phi)$, where I_s is the supercurrent through the junction, I_c is the critical current and ϕ is the so-called Josephson phase which is equal to the difference of the phases of the quantum-mechanical macroscopic wave functions in the electrodes. The Josephson relation for a Josephson π -junction is $I_s = -I_c \sin(\phi) = I_c \sin(\phi + \pi)$, i.e., a π -junction can be considered as a junction with negative critical current or having an additional phase shift of π between the phases of the wave functions (therefore the name). Accordingly, conventional Josephson junctions are sometimes called 0-junctions.

If one considers a 1D long Josephson 0- π -junction (LJJ) made of alternating parts with positive and negative critical currents (0 and π -parts), half-integer ux quanta (semi-uxons²) may spontaneously form at the boundaries between 0 and π regions.

Semi-uxons are very interesting objects which are not yet studied in detail, first of all because up to now it was rather difficult to fabricate 0- π -junctions. Recently several groups succeeded to demonstrate 0- π -junctions based on various technologies: YBa₂Cu₃O₇-Nb ramp zigzags^{3,4}, grain boundary junctions based on tri- and tetra-crystals^{5,6} and Nb junctions based on an artificially created discontinuity⁷. Both 0 and π junctions from the Superconductor-Ferromagnet-Superconductor family were demonstrated by several groups^{8,9,10} but a 0- π -LJJ was not reported yet. Semi-uxons were observed using SQUID microscopy in different types of 0- π -LJJ^{4,11,12,13}.

A single semi-uxon, formed in a LJJ of length L_j with one 0- π -boundary, is pinned at this 0- π -boundary^{14,15} and can have positive or negative polarity carrying the ux $\pm \phi_0/2$ or $\phi_0/2$, respectively. The bias

current from 0 up to $\pm I_c$ ($I_c = j_c w L$ is the "intrinsic" critical current, w is the junction width) cannot move the semi-uxon but just changes its shape¹⁴. This property suggests to use semi-uxons in information storage devices, classical or quantum.

In the classical regime the polarity of a semi-uxon (positive or negative) will encode a logical 0 or 1. The information encoding using semi-uxons is somewhat more robust than using uxons because semi-uxons cannot "escape" as they are pinned at the discontinuity point. The switching between these states can be done by injecting a single ux quantum of proper polarity into the junction.

In the quantum limit a semi-uxon having two possible polarities is similar to a spin with two possible orientations (up or down). Therefore we often use spin notation to denote the polarity of the semi-uxon, i.e., " \uparrow " or " \downarrow ". Analogously, we denote the polarity of a uxon as " \ast " or " $\#$ ". It seems that a semi-uxon is an interesting candidate to realize a qubit. It still remains a challenging task to

find out whether the semi-uxon may stay in the superposition of both states and perform quantum tunneling between them or not. In comparison with a uxon based qubit the one based on a semi-uxon should be more robust as both " \uparrow " and " \downarrow " states represent the ground state of the system, while the uxon of any polarity is an excited state, the ground state being the one with constant phase.

For both quantum and classical bits one needs a way to determine the final state of the semi-uxon, i.e., read out its polarity. Imagine the simplest situation: a single semi-uxon of unknown polarity in an annular LJJ⁷. Let us inject a uxon of a certain polarity into this Josephson ring somewhere far from the semi-uxon position, e.g., using a pair of current injectors¹⁶. If the polarities of the uxon and of the semi-uxon are different, the "annihilation" between uxon and semi-uxon will result in a

pinned semi-uxon of the opposite polarity (we assume that the bias current is zero during uxon injection). The I(V) characteristic (IVC) of the resulting state has a rather large maximum supercurrent (depinning current of a semi-uxon) $I_c^* = 2I_c$ in normalized units ($I = I/I_c$). On the other hand, if the uxon and the semi-uxon are of the same polarity, no "annihilation" takes place. If the bias current is applied, the uxon starts moving passing through the semi-uxon resulting in a finite voltage across the LJJ and rather low I_c^* . In this case the depinning current I_c^* is determined by the repulsion force between uxon and semi-uxon. The uxon should overcome this pinning by the semi-uxon to start moving around the ring.

In this paper we propose a technique to test the polarity of semi-uxons by introducing test uxons into the Josephson ring. Measuring the current-voltage characteristic we can determine the polarity of semi-uxon(s) before the uxon was introduced. We also study resulting states which have different critical (depinning) currents and different dynamics.

In section II we introduce the model which is used for numerical simulations. The numerical results are presented and discussed in section III. Section IV concludes this work.

II. THE MODEL

The dynamics of the Josephson phase in a LJJ consisting of alternating 0 and π parts can be described by the 1D perturbed sine-Gordon equation¹

$$\frac{\partial^2 \phi}{\partial x^2} - \frac{\partial^2 \phi}{\partial t^2} + \sin \phi = \frac{\partial \phi}{\partial t} + \sum_n \delta(x - x_n) \phi(x); \quad (1)$$

where $\phi(x;t)$ is the Josephson phase and subscripts x and t denote the derivatives with respect to coordinate x and time t . In Eq. (1) the spatial coordinate is normalized to the Josephson penetration depth λ_J and the time is normalized to the inverse plasma frequency ω_p^{-1} ; $\gamma = 1/\omega_p^2$ is the dimensionless damping (ω_p is the McCumber-Stewart parameter); $j = j_c$ is the external bias current density normalized to the critical current density of the junction. The function $\phi(x)$ is a step function which is π -discontinuous at all points where 0 and π parts join and is a constant equal to ϕ_n within each part (n is an integer). For example, $\phi(x)$ can be equal to zero along all 0-parts and π along all π -parts.

It is clear from Eq. (1) that $\phi(x)$ is also π -discontinuous at the same points as $\phi(x)$. Therefore, we often call the points where 0 and π parts join phase discontinuity points.

Note that to describe 0- π LJJ's other authors^{2,17,18} often use directly the equation with alternating critical current density written for the continuous phase $\phi(x;t)$

$$\frac{\partial^2 \phi}{\partial x^2} - \frac{\partial^2 \phi}{\partial t^2} + \sin \phi = \frac{\partial \phi}{\partial t} + \sum_n \delta(x - x_n) \phi(x); \quad (2)$$

The Eqs. (1) and (2) are, actually, equivalent and one

can be obtained from the other by substitution $\phi(x;t) = \phi(x;t) + \phi(x)^1$.

In case of an annular LJJ one should use periodic boundary conditions (b.c.) to solve Eq. (1) or (2). In the case of a conventional annular LJJ without phase discontinuities the boundary conditions are expressed as follows

$$\phi(L;t) = \phi(0;t) + 2\pi n_F; \quad (3)$$

where n_F is the number of ux quanta (Josephson vortices) trapped in the ring. Note that when there are no discontinuities, so that b.c. (3) holds for ϕ also.

For the case of an annular LJJ with discontinuities the boundary conditions for ϕ are still given by Eq. (3). This can be understood using the following gedanken experiment. Imagine that we start from the state without discontinuities $\phi(x) = 0$. Then we slowly increase a discontinuity, e.g., by using a pair of closely located injectors, at some point $x = x_0$ from the value 0 to some value π . It is clear that the Josephson phase $\phi(x)$ changes somehow on the length scale λ_J in the vicinity of x_0 to compensate (to react on) this discontinuity, e.g., by forming a fractional vortex with the center at $x = x_0$. In any case the phase $\phi(x)$ and its derivative $\phi_x(x)$ are smooth and continuous functions all along the junction except for the point $x = x_0$. Assuming that the discontinuity point does not coincide with $x = 0$ or with $x = L$, we can write $\phi(0) = \phi(L)$ and $\phi_x(0) = \phi_x(L)$. In the presence of additional uxons trapped in the junction we get b.c. (3) even in the presence of the discontinuity points.

The b.c. for ϕ can be written, recalling that $\phi = \phi(x)$

$$\phi(L;t) = \phi(0;t) + \sum n_{SF} + 2\pi n_F; \quad (4)$$

where n_{SF} is the sum of all discontinuities (semi-uxons) in the ring. Note that if

$$\phi(x) = \sum_{i=1}^N \phi_i H(x - x_i); \quad (5)$$

where ϕ_i is the i -th discontinuity and $H(x)$ is a Heaviside step function, the expression for n_{SF} is

$$n_{SF} = \sum_{i=1}^N \phi_i; \quad (6)$$

In this paper we will investigate the following two cases

1. A uxon is injected into the annular LJJ containing a negative semi-uxon, i.e., $n_F = +1$, $n_{SF} = -1$.
2. A uxon is injected into the annular LJJ containing a positive semi-uxon, i.e., $n_F = +1$, $n_{SF} = +1$.

III. NUMERICAL RESULTS

The simulations were performed using StkJJ software¹⁹ and were confirmed by an independently written program²⁸.

We use $\beta = 0.1$ for all results reported here. This value is not very high, so that it allows to observe some dynamics. On the other hand, it is not very low as the majority of 0- junctions has rather high damping. In the case $\beta \ll 1$ the static results related to the reading out the state of a semion hold, but no dynamical effects such as uxon steps can be observed.

In order to visualize and to understand the uxon and semion dynamics we plot their trajectories on the $(x;t)$ plane. Usually, to track the trajectory of a uxon one tracks the trajectory of its center. Since at a given instant of time the phase $\phi(x)$, corresponding to the uxon solution, changes from 0 at $x \neq 1$ to 2π at $x \neq +1$, it is assumed that the center of a uxon coincides with the point where the phase $\phi = \pi$. Since the phase is defined modulo 2π , in the general case the center of uxons is situated at points where $x = 1 + 2k$ with integer k . To distinguish between uxons and anti uxons, we also check the sign of the phase derivative ϕ_x (magnetic field) at the point where $\phi = \pi + 2k$. If the sign is positive, then it is a uxon and we plot its position as a black point on $x(t)$ plane. If $\phi_x < 0$, then we plot it as a gray points on the $x(t)$ plane.

When we deal with semions, the idea is the same, but since the phase of a semion changes from 0 to $(\text{mod } \pi)$ we have to define the centers of semions as the points where $\phi = \pi/2 + k\pi$. The sign of ϕ_x at the points where $\phi = \pi/2 + k\pi$ is used to distinguish between semions of positive and negative polarity. With this definition, every 2-uxon carrying the integer u_0 results in two points on the $x(t)$ plane, i.e., its trajectory will be represented by a double line.

Below we present numerical results obtained for an annular junction of length $L = 8\pi$.

A. One semion in a ring

First we investigate numerically an annular LJJ with only one phase discontinuity point.

Here and below, without losing generality, we assume that the injected uxons have positive polarity $u_F = +1$ in (4)].

1. Negative semion

If initially the semion has negative polarity $u_{SF} = -1$ in (4)] the uxon is attracted by the semion and, in the absence of a bias current, they "annihilate", resulting in a positive semion $u = 1$.

In Fig. 1(a) one can see the "annihilation" process of the semion situated at $x = 3$ and the uxon injected

at $x = 6$ (it corresponds to two lines at $x = 5$ and $x = 7$ at $t = 0$) for zero bias current $I = 0$. If we trace the IVC of the state after annihilation, we get the curve shown in Fig. 2 by solid black symbols. As a horizontal axis we use the uxon velocity u normalized to the Swihart velocity and proportional to the voltage across the junction. In this notation a single uxon has an asymptotic velocity 1, two uxons have $u \neq 2$ as β grows, etc.. At $u = 0$ the state of the system is the semion $u = 1$ with maximum supercurrent (semion depinning current) $I_c = 2I_0 = 0.63^{4,20,21,22}$. When the bias current exceeds this value the system switches to the M ϕ Cumber branch. By sweeping the bias current back one may trace the step with asymptotic velocity $u = 3$, corresponding to the state $u = 4$, which is formed probably due to the topological instability of the solution similar to the formation of zero-field steps in conventional LJJ. The trajectories corresponding to the bias point d can be seen in Fig. 1(d).

What happens if we inject a uxon while having a non-zero bias current? If the bias current as well as the distance between uxon injection point and semion are large enough, the uxon approaches the semion with rather high velocity and annihilation will not take place — the uxon will simply pass through the semion. Thus, injecting a uxon at a finite bias current we can trace an IVC which is shown in Fig. 2 by open symbols. The semion trajectories at the bias points b and c are shown in Fig. 1(b)–(c), accordingly. One can see that in average a semion is shifted by the bias current away from the discontinuity point and oscillates around this new equilibrium position as the uxon bumps it. Comparing Fig. 1(b) and (c), one can also notice that the uxon's double line is more tight in (c) which is a result of relativistic contraction. Note that after the bias current is reduced to zero the annihilation takes place anyway and the system returns to the IVC corresponding to the state $u = 1$, without a moving uxon, so that further sweeping of I shows only the curve drawn by solid black symbols in Fig. 2.

Actually one can also trace the second uxon step with asymptotic velocity $u = 2$. It corresponds to the state $u = 2$ and is shown in Fig. 2 by solid gray symbols. We were able to find this state only starting from the point e at $I = 0.3$ with a uxon situated at $x = 5$ and an anti uxon at $x = 8$. It is impossible to visualize this mode just by sweeping the bias current since this step is shadowed by $u = 1$, $u = 3$ and $u = 4$ steps.

2. Positive semion

Now we consider a semion of a positive polarity initially present in the LJJ. The injected uxon and semion repel each other and no annihilation can occur. Here we use the boundary conditions (4) with $k_F = 1$ and $k_{SF} = 1$ to obtain the IVC. By applying a small bias current we push the uxon along the ring so it approaches

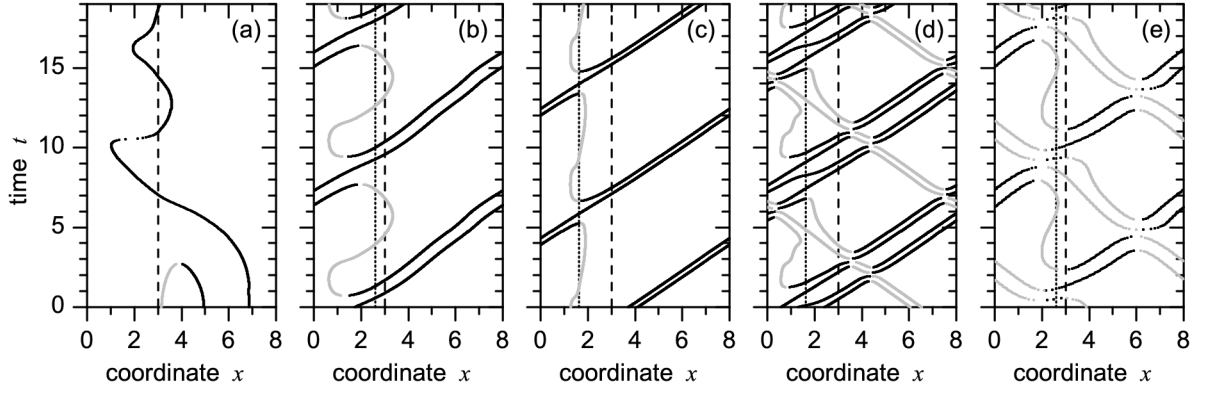


FIG. 1: Trajectories of uxons (double line) and semi-uxons (single line) corresponding to annihilation $++ = -$ at $t = 0$ (a); dynamics in the state $++$ at the first uxon step at $t = 0.3$ (b); at $t = 0.6$ (c); dynamics at the third uxon step (state $++$) at $t = 0.6$ (d); dynamics at the second uxon step (state $++$) at $t = 0.3$. The vertical dashed line shows the position of the discontinuity. The vertical dotted line shows the position of the center of the static semi-uxon at the corresponding bias. In (a) for $t = 0$ both lines coincide.

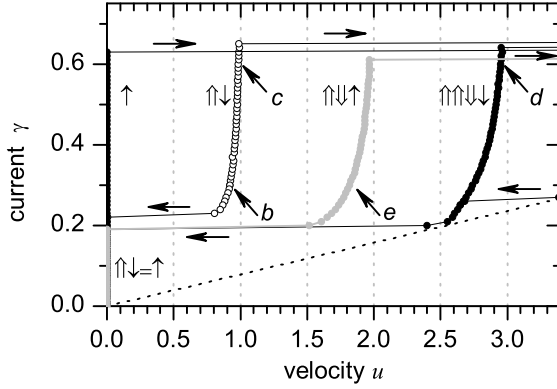


FIG. 2: IVC after injection of a uxon into a 0- LJ containing a semi-uxon of negative polarity. The solid black symbols show the IVC after annihilation, open symbols show the IVC which can be traced if injection takes place at $u > 0.21$. Dotted line shows the position of the Mccumber branch (uniform phase-whirling state).

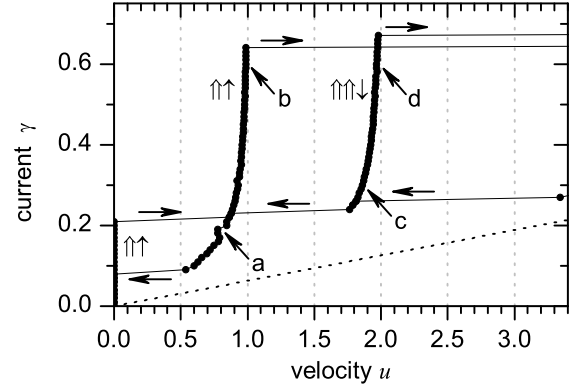


FIG. 3: Current voltage characteristic after injection of uxon into 0- LJ containing a semi-uxon of positive polarity. All (even and odd) uxon steps can be traced. The maximum supercurrent $\gamma_{max} = 0.21$. The trajectories at the bias points a-d are shown in Fig. 4(a)-(d).

the semi-uxon. For a small value of the bias current the situation is static as the driving force of the bias current can be compensated by the repulsion force between the uxon and the semi-uxon. By increasing the bias current, the uxon moves closer to the semi-uxon and at some critical value of the bias current overcomes the maximum possible repulsion force and passes through the semi-uxon. After this, the uxon keeps moving around the ring, bumping the semi-uxon once per cycle. The current voltage characteristic of this state is shown in Fig. 3. One can see that the maximum supercurrent $\gamma_c^* = \frac{2}{3} = 0.21$ (see Appendix A), corresponding to the maximum possible repulsion force between the uxon and the semi-uxon, is considerably smaller than $\gamma_c = 2$ of a single semi-uxon. Thus, the two situations can be distinguished.

The trajectories corresponding to the dynamics of the system are shown in Fig. 4 for several bias points marked in Fig. 3. We see that at the first uxon step, see Fig. 4(b), the uxon (double line) moves progressively colliding with the semi-uxon. The semi-uxon corresponds to a more or less vertical line shifted to the right from the discontinuity point by the bias current. Note, that in Fig. 4(a) we can see essentially the same dynamics, but the semi-uxon is much more delocalized, probably because bias point a corresponds to the resonance which can be seen on the IVC in Fig. 3. We believe that this resonance may be related to the eigenmodes of the semi-uxon and to the Cherenkov emission of the plasma waves which are excited when the uxon periodically bumps the semi-uxon. The emitted plasma wave forms a standing wave which interacts with a uxon and results in the resonance on the IVC.

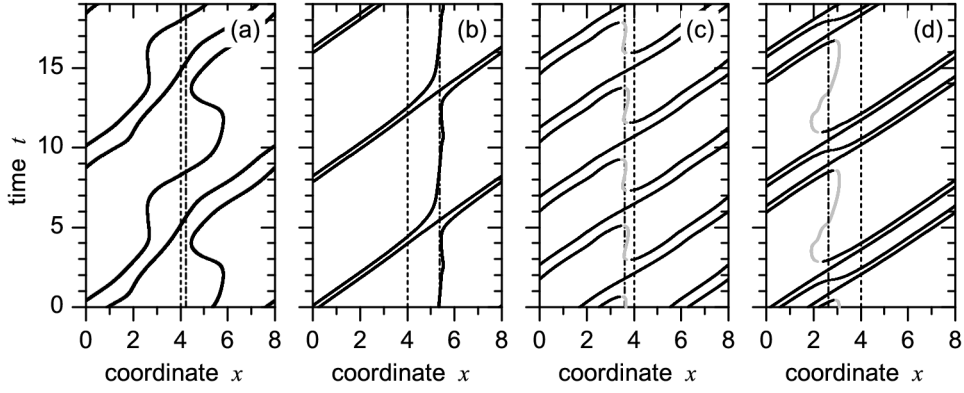


FIG. 4: Trajectories of semi-uxons in the state ** (first uxon step) for $\beta = 0.2$ (a) and $\beta = 0.6$ (b) and in the state **# for $\beta = 0.3$ (c) and $\beta = 0.6$ (d). The vertical dashed line shows the position of the discontinuity. The vertical dotted line shows the position of the center of the static semi-uxon at the corresponding bias. In (a) for $\beta = 0$ both lines coincide.

Thus, the polarity of the semi-uxon can be probed by inserting a test uxon of known polarity and measuring the IVC. If a uxon and a semi-uxon have the same polarity one should expect $I_{max} = \frac{2}{3} I_c \approx 0.21 I_c$ and the appearance of the first uxon step. If a uxon and a semi-uxon have different polarities, one should expect $I_{max} = \frac{2}{3} I_c \approx 0.63 I_c$ and no first uxon step provided the injection was made at $\beta = 0$.

Another difference between these two configurations is the value of the retrapping current I_r . As one can see from Figs. 2 and 3 the value of I_r in the **# = " state is at least twice larger than for the ** state.

An interesting observation can be made, if we trace all uxon branches of the IVC. In a usual annular LJJ with only one trapped uxon (without a semi-uxon) one can observe uxon steps at $V = nV_1$ with only odd numbers n : the first one appears due to the motion of a single uxon, the third one corresponds to an additional uxon-anti uxon pair generated, the fifth one to two uxon-anti uxon pairs, etc..

In an annular LJJ containing a uxon and a semi-uxon of the same polarity the situation is different. One can observe uxon steps with any integer n . This is especially easy to observe for the ** state. The reason for this becomes clear after analysis of the trajectories shown in Fig. 4 for several bias points marked in Fig. 3.

We see that at the second step, there are two positive uxons moving in the same direction and the semi-uxon became of negative polarity **#. This means that the semi-uxon flipped, and has emitted one positive uxon | the process opposite to annihilation. Now, since there are two uxons which can move and one negative semi-uxon which cannot, the asymptotic voltage of the step is equal to $2V_1$. Still, the system can generate uxon-anti uxon pairs which, together with semi-uxon flipping, will result in uxon steps for all integer n .

Actually, a similar effect can be observed when initially the semi-uxon had negative polarity. Then starting from the state " one could trace the uxon steps corresponding to the states **#, **+, **+# (see Fig. 2). The trajectories

for some of the bias points can be seen in Fig. 1.

We also note that when the semi-uxon polarity changes, the shift of the average position of the semi-uxon changes too. This can be visualized using low temperature scanning electron microscopy²³.

Analyzing the trajectories while the bias point moves along the second uxon step we discovered that the two uxons are moving more or less equidistantly at a low value of the bias current, i.e., at the bottom of the step, as can be seen in Fig. 4(c). When the bias current increases up to $0.45 :: 0.50$ or above, the uxons bunch together as shown in Fig. 4(d). The bunching appears because the plasma waves, emitted during uxon-semi-uxon collisions, result in an effective attracting potential between two uxons. We do not discuss this phenomenon in detail here, but note that similar bunching was observed in JJ arrays²⁴ or in stacks of LJJs²⁵. In our case, the role of periodic obstacle is played by a semi-uxon. Generally speaking, the plasma wave emission has a Cherenkov origin and is simply related to the peculiar dispersion relation for plasma waves in the system under question²⁶.

B. Two semi-uxons in a ring

In the case of more than one semi-uxon of unknown polarity, the above read out procedure cannot give information on the polarity of each of the semi-uxons, but allows to distinguish between states (a) " ", (b) ##, and (c) "# or "#. In other words, we can find out the total uxon hold by semi-uxons. Injecting the first uxon in a similar fashion as above, we measure the IVC. If the critical current is low, the uxon does not annihilate with semi-uxons and keeps moving around the ring. This can happen only if in the initial state both semi-uxons had the same polarity as the injected uxon. If, after injection of a uxon, I_c is still high, this means that the injected uxon has flipped one of the semi-uxons. In this

case we inject a second uxon and so on. If I_c becomes lower after the first injection, the initial state has been "0"; if I_c becomes lower after second injection, the initial state has been "# or #"; and if I_c becomes lower after the third injection, the initial state has been "##".

IV. CONCLUSIONS

We have shown that by introducing a test uxon of known polarity into the LJJ with a semi-uxon of unknown polarity we can destructively read out the semi-uxon state. In principle, the read out can be made non-destructive, if after reading out the semi-uxon state we introduce another uxon of opposite polarity so that the system returns to its initial state (as before read out) as a result of uxon-uxon or uxon-semi-uxon annihilation. In case of two or more semi-uxons one can read out the total number of positive and negative semi-uxons. This technique is also applicable to arbitrary fractional vortices, but not very close to $\nu = 0$ or $\nu = 2$ where depinning currents for both $N = 0$ and $N = 1$ approach zero.

We have also investigated uxon steps in an annular LJJ with a π -discontinuity. We found that one can trace the uxon steps corresponding to all integer n , instead of only odd n like in conventional LJJ with one trapped uxon. We have observed a smooth transition to the state of two bunched uxons in the $**\#$ state.

Further, in appendix A we have derived the Eq. (A 9) which gives the depinning current of N uxons pinned by an arbitrary π -vortex. We discovered that the biggest obstacle for a uxon is a fractional $1/2$ -vortex with $\nu = 0.861$ rather than a semi-uxon. The formula (A 10) allows to compute the size ν_N of the fractional vortex which is the biggest obstacle for N uxons trying to pass it.

Acknowledgments

E.G. thanks H. Susanto and S. van Gils for fruitful discussions and hospitality during his visit to University of Twente. This work was supported by the Deutsche Forschungsgemeinschaft, and by the ESF programs "Vortex" and "Pi-shift".

APPENDIX A: DEPINNING OF FLUXONS BY AN ARBITRARY FRACTIONAL VORTEX

Since one can study experimentally arbitrary π -vortices⁷, here we calculate the depinning current for a chain of N uxons that are pinned by and are trying to pass an arbitrary π -vortex in a LJJ of infinite length.

The static version of Eq. (2) for arbitrary discontinuity is:

$$x_N = \sin[\phi(x)] \quad ; \quad (A 1)$$

where

$$\phi(x) = \begin{cases} 0 & \text{for } x < 0; \\ \pi & \text{for } x > 0 \end{cases}$$

We write separately the Eqs. for the part of the junction to the left and to the right from discontinuity, situated at $x = 0$. After integration one arrives to the following two equations.

$$y_1(x) = \frac{1}{2} \frac{C_1(x) \cos(\phi(x))}{C_2(x) \cos(\phi(x))} \quad ; \quad x < 0; \quad (A 2a)$$

$$y_2(x) = \frac{1}{2} \frac{C_1(x) \cos(\phi(x))}{C_2(x) \cos(\phi(x))} \quad ; \quad x > 0 \quad (A 2b)$$

Assuming that

$$x(1) = 0; \quad (A 3)$$

$$\phi(1) = \arcsin \nu; \quad (A 4)$$

$$(\nu + 1) = \arcsin \nu + 2N + \pi; \quad (A 5)$$

we arrive to the following expressions for C_1 and C_2 :

$$C_1(x) = \frac{1}{1 - \nu^2 + \arcsin \nu} \quad ; \quad (A 6)$$

$$C_2(x) = \frac{1}{1 - \nu^2 + \arcsin \nu + (2N + \pi)} \quad ; \quad (A 7)$$

We use the phase plane analysis¹⁵ to find possible static configurations. The trajectories on the phase plane $y_{1,2}(x)$ corresponding to Eqs. (A 2) are shown in Fig. 5 for $\nu = 0$, $\nu < \nu_c$ and $\nu = \nu_c$. At $t = 0$ the uxon and fractional vortex are separated by a large distance. The uxon corresponds to the trajectory between point L ($x = -1$) and point M. The fractional vortex corresponds to the trajectory between point M and point R ($x = +1$) and contains a point P where the black and gray trajectories intersect, i.e., the phase crosses the 0- π boundary. From Fig. 5(a)-(c) one can see that with increasing ν the intersection point P shifts until, at the critical value of $\nu = \nu_c$ the trajectories just touch each other at point P, as shown in Fig. 5(c). For larger ν , no intersection is possible and the static solution does not exist.

The critical value of ν at which the switching between trajectories is still possible is defined by the following conditions:

$$y_1(x) = y_2(x); y_1'(x) = y_2'(x); \quad (A 8)$$

This conditions are satisfied for $\nu = \frac{1}{2}(3 + \pi)$, which leads us to the final result:

$$\nu_c = \frac{2}{2N + \pi} \sin \frac{\pi}{2} \quad (A 9)$$

The plot of this dependence for different N is shown in Fig. 6. The $\nu_c(x)$ has reasonable limiting behavior (absence of pinning for $N > 0$) for $\nu \rightarrow 0$ and $\nu \rightarrow 2$. For depinning of a uxon ($N = 1$) by a semi-uxon, $\nu_c = 2/3 \approx 0.67$. It is interesting that $\nu_c(x)$ has a

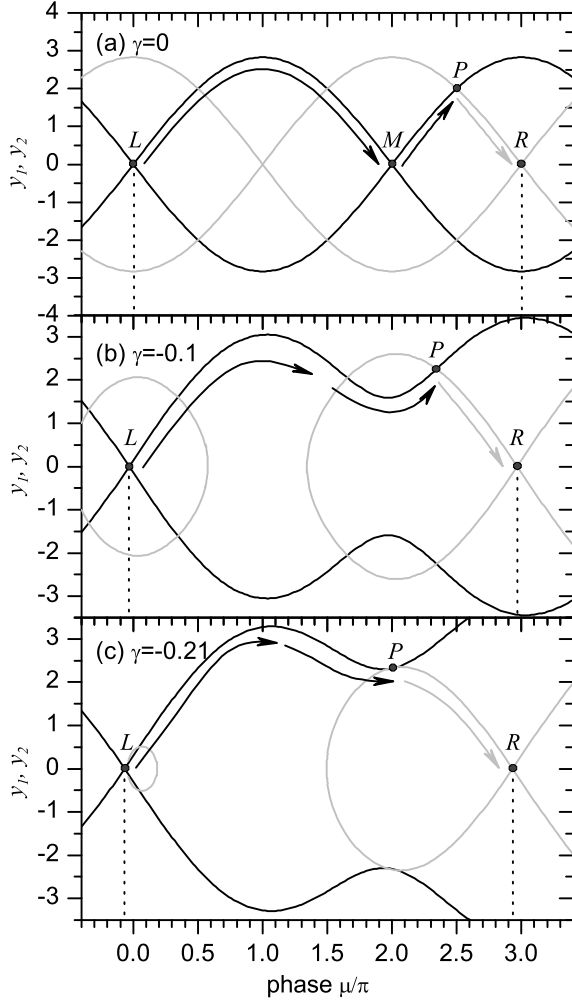


FIG. 5: The trajectories on the phase plane corresponding to Eqs. (A 2). Black color corresponds to y_1 (0-part), the gray color corresponds to y_2 (π -part). The trajectories are presented for a π -vortex pinned by a $\pi/2$ -vortex ($N = 1$, $\gamma = 0$) and (a) $\gamma = 0$, (b) $\gamma = -0.1$ and (c) $\gamma = -0.21$. Arrows are shown to guide the eye. Arrows show the path which corresponds to going from $x = -1$ (point L) to $x = +1$ (point R).

maximum not at $\mu = 0$ but a bit shifted, at $\mu_1 = 0.861$, i.e., a $\pi/2$ -vortex is the biggest obstacle for a π -vortex. For two and three $\pi/2$ -vortices the biggest obstacles are vortices with $\mu_2 = 0.918$ and $\mu_3 = 0.942$. All μ_N can be found from the equation

$$\tan \frac{N}{2} = \frac{N}{2} + N : \quad (\text{A } 10)$$

Note, that in the limit $N \rightarrow 1$, $N \rightarrow \infty$.

Our result (A 9) is also valid in the case $N = 0$ and gives the "depinning" current of the π -vortex itself. The result (A 9) coincides with the expression obtained recently for the critical current of an annular junction in the presence of a π -discontinuity of the phase (current dipole) created by injectors²⁰. In fact one can even say that our result

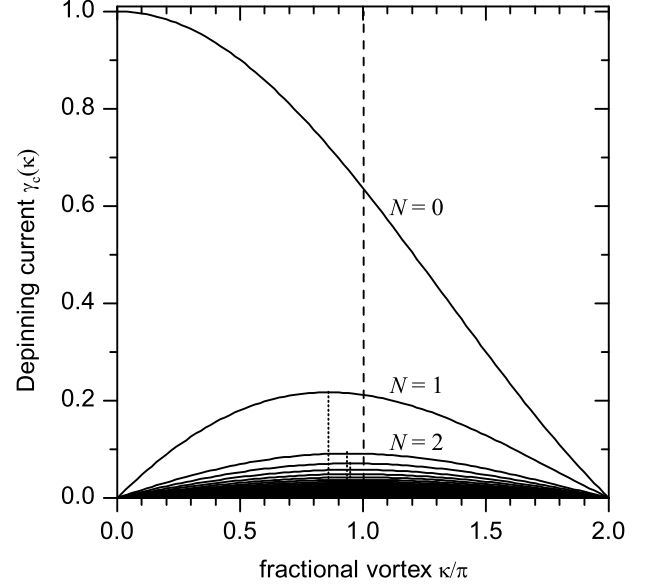


FIG. 6: The dependence $c_c(\kappa)$ calculated for different N using Eq. (A 9). The dashed line shows $\mu = 0$ corresponding to the π -vortex. Three dotted lines show the values μ_1 , μ_2 and μ_3 which correspond to the fractional vortices which cause the maximum possible pinning for $N = 1; 2; 3$ vortices.

(A 9) and the one of Ref. 20 are the same at least if one considers an annular LJJ. In fact, if we denote $\mu_0 = 2N + \mu$, we can rewrite (A 9) as

$$c_c(\mu_0) = \frac{2 \sin \frac{\mu_0}{2}}{\mu_0}; \quad (\text{A } 11)$$

exactly as in Ref. 20. Physically this means that when one creates a large discontinuity $\mu_0 = 2N + \mu$ in an annular LJJ, it automatically relaxes into N $\pi/2$ -vortices trying to pass through the fractional π -vortex under the action of bias current. The interesting result is that the Eq. (A 9) for an infinitely long linear junction and Eq. (A 11) for an annular one coincide regardless of "vortex crowding" which may take place in annular LJJ because of its finite length.

Electronic address: gold@uni-tuebingen.de;
URL: http://www.geocities.com/e_goldobin

¹ E. G. Goldobin, D. Koelle, and R. Kleiner, Phys. Rev. B 66, 100508 (2002).

² J. H. Xu, J. H. Miller, and C. S. Ting, Phys. Rev. B 51, 11958 (1995).

³ H.-J. H. Smilde, A. Riando, D. H. A. Blank, G. J. Gerrensma, H. Hilgkamp, and H. Rogalla, Phys. Rev. Lett.

- 88, 057004 (2002), PDF.
- ⁴ H. H. Ilgenkamp, A. Riando, H.-J. H. Smilde, D. H. A. Blank, G. Rijnders, H. Rogalla, J. R. Kirtley, and C. C. T. Sui, *Nature* 422, 50 (2003).
 - ⁵ B. Chesca, R. R. Schulz, B. Goetz, C. W. Schneider, H. H. Ilgenkamp, and J. Mannhart, *Phys. Rev. Lett.* 88, 177003 (2002).
 - ⁶ B. Chesca, K. Ehrhardt, M. Mole, R. Straub, D. Koelle, R. Kleiner, and A. Tsukada, *Phys. Rev. Lett.* 90, 057004 (2003).
 - ⁷ E. Goldobin, A. Sterck, T. Gaber, D. Koelle, and R. Kleiner, *Phys. Rev. Lett.* 92 (2004).
 - ⁸ T. Kontos, M. Aprili, J. Lesueur, F. Genêt, B. Stephanidis, and R. Boursier, *Phys. Rev. Lett.* 89, 137007 (2002).
 - ⁹ V. V. Ryazanov, V. A. Oboznov, A. Y. Rusanov, A. V. Veretennikov, A. A. Golubov, and J. Aarts, *Phys. Rev. Lett.* 86, 2427 (2001).
 - ¹⁰ Y. Blum, A. Tsukernik, M. Karpovskii, and A. Palevski, *Phys. Rev. Lett.* 89 (2002).
 - ¹¹ J. R. Kirtley, C. C. T. Sui, and K. A. Moler, *Science* 285, 1373 (1999).
 - ¹² J. R. Kirtley, C. C. T. Sui, M. Rupp, J. Z. Sun, L. S. Yu-Jahnes, A. Gupta, M. B. Ketchen, K. A. Moler, and M. Bhushan, *Phys. Rev. Lett.* 76, 1336 (1996).
 - ¹³ R. G. Mints, I. Papiashvili, J. R. Kirtley, H. H. Ilgenkamp, G. Hamerl, and J. Mannhart, *Phys. Rev. Lett.* 89, 067004 (2002).
 - ¹⁴ E. Goldobin, D. Koelle, and R. Kleiner, *Phys. Rev. B* 67, 224515 (2003), cond-mat/0209214.
 - ¹⁵ H. Susanto, S. A. van Gils, T. P. P. V. Isser, A. Riando, H.-J. H. Smilde, and H. H. Ilgenkamp, *Phys. Rev. B* 68, 104501 (2003).
 - ¹⁶ A. V. Ustinov, *Appl. Phys. Lett.* 80, 3153 (2002).
 - ¹⁷ J. R. Kirtley, K. A. Moler, and D. J. Scalapino, *Phys. Rev. B* 56, 886 (1997).
 - ¹⁸ A. Buzdin and A. E. Koshelev, *Phys. Rev. B* 67, 220504 (pages 4) (2003), cond-mat/0305142.
 - ¹⁹ E. Goldobin (2003), URL <http://www.geocities.com/SiliconValley/Heights/7318/StkJJ.htm>.
 - ²⁰ B. A. Malomed and A. V. Ustinov, *Phys. Rev. B* 69, 064502 (pages 8) (2004), cond-mat/0310595, URL <http://link.aps.org/abstract/PRB/v69/e064502>.
 - ²¹ T. Kato and M. Imada, *J. Phys. Soc. Jpn.* 66, 1445 (1997), cond-mat/9701147.
 - ²² A. Zenchuk and E. Goldobin, *Phys. Rev. B* 69, 024515 (2004), nlin.ps/0304053.
 - ²³ A. Laub, T. Doderer, S. G. Lachenmann, R. P. Huebener, and V. A. Oboznov, *Phys. Rev. Lett.* 75, 1372 (1995).
 - ²⁴ A. V. Ustinov, B. A. Malomed, and S. Sakai, *Phys. Rev. B* 57, 11691 (1998).
 - ²⁵ E. Goldobin, A. Waltra, N. Thyssen, and A. V. Ustinov, *Phys. Rev. B* 57, 130 (1998).
 - ²⁶ E. Goldobin, A. Waltra, and A. V. Ustinov, *J. Low Temp. Phys.* 119, 589 (2000).
 - ²⁷ We note that such annular junctions cannot be constructed using natural 0- junctions because one part cannot be simultaneously 0 and . There should be always an even number of 0- -joints. In an experiment the proposed situation can be realized using artificial 0- -LJJ based on conventional superconductors with a pair of -injectors⁷. This case of only one discontinuity in a ring is very interesting as it allows to go beyond the possibilities offered by nature.
 - ²⁸ written by N. Stefanakis